Ice cap melting and low-viscosity crustal root explain the narrow geodetic uplift of the Western Alps

Jean Chery, Manon Genti, Philippe Vernant

AGU PUBLICATIONS

Geophysical Research Letters

RESEARCH LETTER
10.1002/2016GL067821

Key Points:
- Explanation for the geodetic uplift of the Alps
- Revisit the relation between deglaciation and uplift
- Pointing out the key role of rheology on strain

Correspondence to:
J. Chéry,
jchery@um2.fr

Citation:
Chéry, J., M. Genti, and P. Vernant (2016), Ice cap melting and low-viscosity crustal root explain the narrow geodetic uplift of the Western Alps, *Geophys. Res. Lett., 43*, 3193–3200, doi:10.1002/2016GL067821.

Received 15 JAN 2016
Accepted 24 MAR 2016
Accepted article online 30 MAR 2016
Published online 6 APR 2016

Ice cap melting and low-viscosity crustal root explain the narrow geodetic uplift of the Western Alps

J. Chéry[1], M. Genti[1], and P. Vernant[1]

[1]Geosciences Montpellier, CNRS and Université de Montpellier, Montpellier, France

Abstract More than 10 years of geodetic measurements demonstrate an uplift rate of 1–3 mm/yr of the high topography region of the Western Alps. By contrast, no significant horizontal motion has been detected. Two uplift mechanisms have been proposed: (1) the isostatic response to denudation responsible for only a fraction of the observed uplift and (2) the rebound induced by the Wurmian ice cap melting which predicts a broader uplifting region than the one evidenced by geodetic observations. Using a numerical model to fit the geodetic data, we show that a crustal viscosity contrast between the foreland and the central part of the Alps, the latter being weaker with a viscosity of 10^{21} Pa s, is needed. The vertical rates are enhanced if the strong uppermost mantle beneath the Moho is interrupted across the Alps, therefore allowing a weak vertical rheological anomaly over the entire lithosphere.

1. Geodetic Uplift of the Alps

The central and Western Alps display a moderate seismicity mostly associated with normal faulting [*Tricart et al*., 2004; *Sue et al*., 2007]. This belt-perpendicular extension could be attributed to a topography collapse related to the gravitational potential energy of the mountain [*Selverstone*, 2005]. In the case of the Alps, gravitational spreading seems to be incompatible with leveling and Global Navigation Satellite Systems (GNSS) observations that reveal a present-day uplift from 1 and up to 3 mm/yr [*Schaer and Jeanrichard*, 1974; *Serpelloni et al*., 2013]. Moreover, horizontal geodetic motion is below 0.5 mm/yr [*Nocquet*, 2012], suggesting that vertical uplift rates do not find their origin in horizontal plate motion. As shown in Figure 1, uplifted areas correlate well with high (>1500 m) topography except in the Southern Alps where they remain close to zero. If this vertical motion is a persistent feature of the Alpine deformation, at least three processes can be invoked to explain this uplift.

1. A slab detachment or a delamination process could result into an isostatic disequilibrium and induce a vertical motion. Such a process could be at work in the Carpathians [*Joó*, 1992] and could occur in the Alps [*Lyon-Caen and Molnar*, 1989; *Singer et al*., 2014; *Fox et al*., 2015]. However, realistic mechanical modeling of the alpine deformation indicates that a large part of the root is in local isostatic equilibrium [*Burov et al*., 1999], therefore precluding large tractions associated to body forces from the uppermost mantle.
2. Erosional processes could lead to an isostatic response. Denudation rates of 0.4–1.4 mm/yr are provided by ^{10}Be cosmogenic analysis for several watershed [*Brocard et al*., 2003; *Hinderer et al*., 2010; *Wittmann et al*., 2007]. Using these denudation rates and a 10 km thick elastic plate model provides rock uplift rates up to 0.8 mm/yr, hence significantly smaller than the geodetic values [*Champagnac et al*., 2009].
3. Mass unloading associated to the disappearance of the large Pleistocene ice cover could contribute to present-day uplift [*Gudmundsson*, 1994]. However, large-scale plate models [*Stocchi et al*., 2005] predict a broad uplift across the Alps, with a maximum uplift rate reaching 0.2 mm/yr, far smaller than the geodetic values. In contrast to the hypothesis of *Champagnac et al*. [2009], a thick lithospheric plate of 120 km was used by *Stocchi et al*. [2005] to model the response to the deglaciation. Another contribution for present-day uplift could arise from ice unloading following Little Ice Age. Using a thin viscoelastic plate model, *Barletta et al*. [2006] calculated an average uplift value of 0.1–0.2 mm/yr over the whole alpine belt with local maximum uplift rates up to 0.8 mm/yr at the vicinity of the largest glaciers.

An appealing argument in favor of a glacial origin for the triggering of geodetic uplift comes from the correlation between maximum ice cap thickness, geodetic uplift, and high elevations. Indeed, very low, if any, vertical uplift occurs in the Southern Alps where the Wurm glaciation was very mild. By contrast, maximum geodetic uplift occurs in Switzerland where an average ice thickness of 1 km has been documented. Using

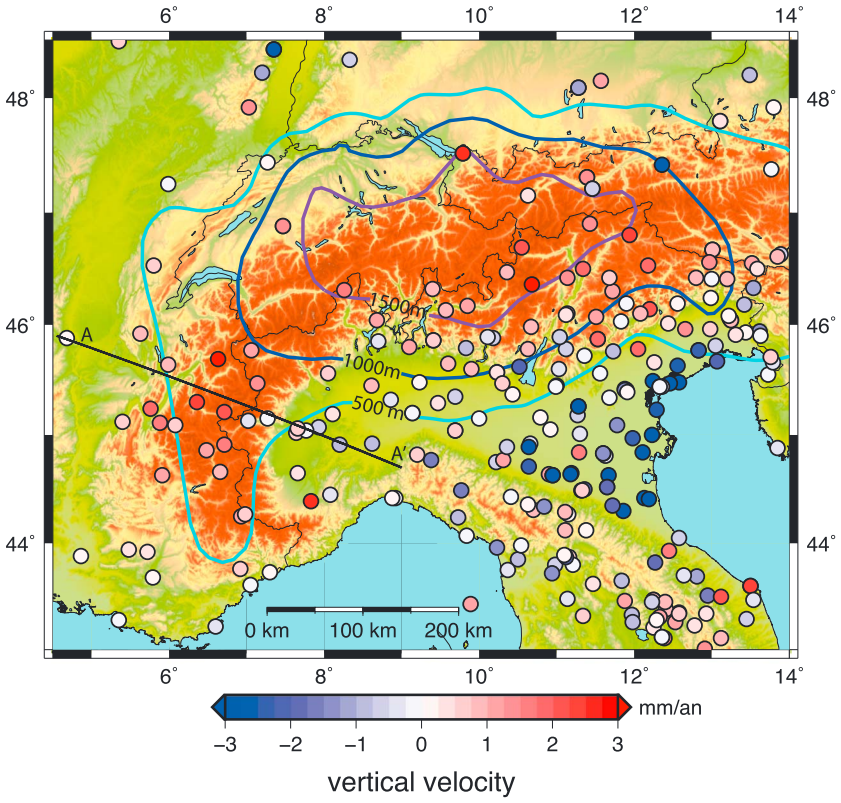

Figure 1. Isopachs of Wurmiam ice cap [from *Stocchi et al.*, 2005] and vertical geodetic motion of the Alps [from *Serpelloni et al.*, 2013].

a 2-D viscoelastic model, we revisit the impact of Holocene deglaciation on vertical motion and we show the strong impact of crustal rheology on the present-day deformation of the Alps.

2. Modeling the Rheological Structure of the Alps

The lithosphere rheology and temperature have profound implications on mountain deformation processes as suggested by modeling studies [e.g., *Beaumont et al.*, 1994]. An open question is the strength of the uppermost mantle, which has been claimed weak [*Maggi et al.*, 2000; *Jackson et al.*, 2004] or strong [*Burov and Watts*, 2006]. Also, the lower crust rheology remains poorly known because of its variable composition [*Lyon-Caen and Molnar*, 1989; *Burgmann and Dresen*, 2008]. We build a mechanical model compatible with our present-day knowledge of the lithosphere rheology, complemented with available geophysical observations in the Alps and its surroundings (Figure 2). Contrary to *Stocchi et al.* [2005] layered model, we consider that the Alps encompass a large rheological heterogeneity mostly due to thermal processes. A simple calculation accounting for the thickened radiogenic crust (reaching up to 60 km) suggests that heat flow may reach 90–100 mW/m^2 in the inner part of the Alps. Such high values are compatible with measurements [*Majorowicz and Wybraniec*, 2010] and a 350°C isotherm at 10–15 km depth. Because it has been shown a correlation between surface heat flow and earthquake depth distribution [*Meissner and Strehlau*, 1982; *Sibson*, 1982], the depth of the seismicity in the Alps [*Deichmann*, 2003; *Béthoux et al.*, 2007; *Lenhardt et al.*, 2007] provides an indirect information on the thermal state of the upper crust. These studies indicate that most of the crustal seismicity occurs between 0 and 12 km depths in the inner Alps. By contrast, seismicity of the Alpine foreland reaches the deepest parts of the crust. We therefore assume that the Alpine foreland crust can be modeled using an entirely elastic crust of 30 km thickness, and we reduce this elastic thickness to 10 km for the inner Alps following Champagnac's hypothesis. Below 10 km, we assume that crustal deformation occurs by thermally activated viscous processes that we model using a linear viscoelastic Maxwell model. Because lower crustal rheology is expected to vary largely as a function of composition and temperature, we test a wide viscosity range (10^{20}–10^{23} Pa s). Below the

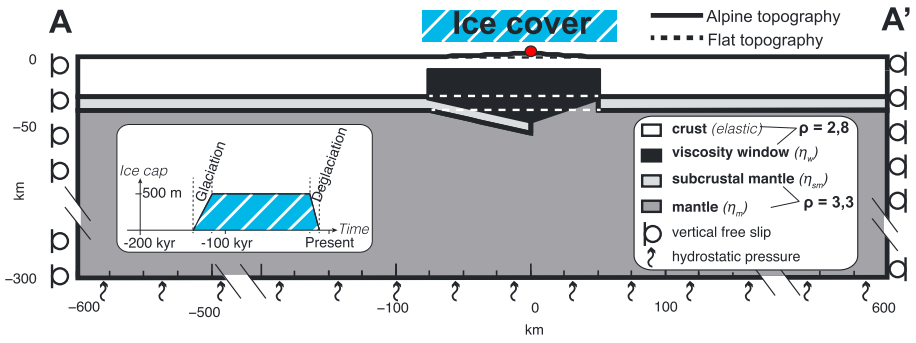

Figure 2. Model setting of alpine deglaciation. Lateral boundary conditions are set to zero for horizontal velocity component but are free to move vertically. Hydrostatic pressure is set at the base of the model. The ice cover change shown in the inset is modeled using a dynamic mesh update for the topography.

crust, the strength of the continental uppermost mantle has been the locus of much debate. This part of the lithosphere has been considered stronger than the lower crust [*Brace and Kohlstedt*, 1980], but some authors provided contrary arguments based on seismicity and flexural analysis [*Maggi et al.*, 2000]. For the European plate, this subcrustal plate may correspond to the remnant of the continental mantle subduction that ceased at the end of the Miocene [*Lardeaux et al.*, 2006]. We assume that this subduction should be guided by a strong uppermost mantle, and we use a viscosity of 10^{24} Pa s. At greater depth, the upper mantle viscosity is relatively well constrained by postglacial rebound observations and models [*Milne et al.*, 2001] and we test here a viscosity range between 10^{20} and 10^{21} Pa s.

We model the deformation and associated uplift of this Alpine rheological model under the weight of Wurmian glaciation. Because the model is submitted to body forces, the resulting deformation occurs in response from both rheological stratification and density variation associated with topography and crustal root. In order to separate these deformation sources, we also run a model similar to the one in Figure 2 (named Alpine model) but with a flat topography and Moho (named Flat model). According to *Stocchi et al.* [2005], we assume for both models that the surface is covered by an average ice thickness reaching 500 m over a width of 100 km (Figure 2). Although the chronology of formation and melting of Wurmian ice cap remain uncertain, we used the synthesis provided by these authors to setup ice thickness evolution of our models. The experiment accounts for model equilibration (−200 to −140 kyr), onset of glaciation (−140 to −120 kyr), and ice cap retreat (−21 to −10 kyr).

3. Results

We present in Table 1 and Figures 3 and 4 the results associated with the most significant experiments. Uplift rate profiles (Figure 3) and values for the central part of the range (0 km) and the foreland (−75 km) for the Alpine and flat topography models are similar. For low-viscosity Alpine models the final profiles suffer of the initial instability between the topography and the crustal root. It induces for case d (10^{20} Pa s for crust

Table 1. Rheological Layering[a]

Case	Crustal Root Viscosity (Pa s)	Upper Mantle Viscosity (Pa s)	Broken Uppermost Mantle	Uplift (mm/yr)			
				Alpine Model		Flat Model	
				−75 km	0 km	−75 km	0 km
a	10^{23}	10^{20}	Yes	0.0	0.0	0.0	0.1
b	10^{22}	10^{20}	Yes	0.0	0.4	0.0	0.5
c	10^{21}	10^{20}	Yes	−0.1	1.8	−0.2	1.3
d	10^{20}	10^{20}	Yes	1.2	1.4	−0.2	0.8
e	10^{21}	10^{21}	Yes	1.0	2.6	1.0	2.5
f	10^{21}	10^{20}	No	0.0	0.7	−0.4	0.8

[a]Rheological layering and present-day uplift of experiments; Uplift values are given for mountain center (x = 0 km) and foreland (x = -75 km) (see Figures 2 and 3 for location).

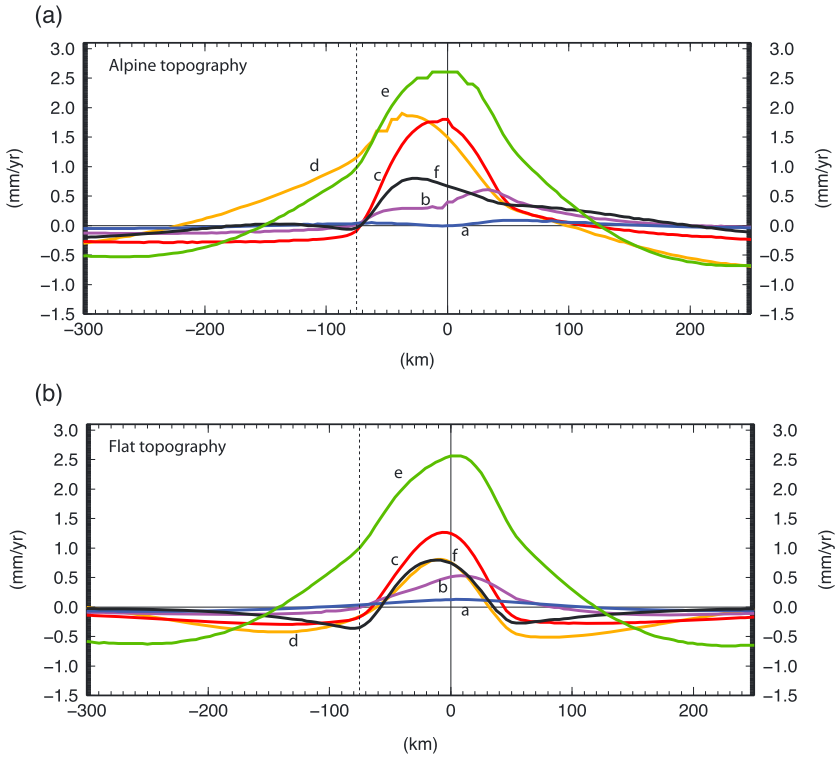

Figure 3. Uplift rate versus horizontal distance for experiments. (a) Alpine model (with topography and crustal root). (b) Flat model (no topography and no crustal root). See Table 1 for rheological parameters associated with the labeled curves.

and mantle) an asymmetric vertical response to deglaciation. These observations raise the question on how to maintain a long-term topography with a low viscous crustal root.

Among the tested viscosities, only a low viscosity of 10^{21} Pa s for the crustal root (Figure 3, case c) leads to a high and localized uplift coherent with the geodetic data. The good spatial correlation between ice load and uplift is due to the low rigidity of the Alps in which its strength is mostly restricted to the elastic upper crust. Higher viscosities of 10^{22} and 10^{23} Pa s (Figure 3a, cases b and a) produce a moderate and distributed uplift with maximum values lower than 0.5 mm/yr. Because a viscous lower crust of 10^{23} Pa s is nearly equivalent to an elastic layer, this small and widespread uplift is equivalent to a flexural response of a 40 km thick elastic crustal plate.

In addition to crustal root viscosity, the lateral continuity of the uppermost mantle also impacts the present-day uplift pattern. Assuming a continuous lid of a strong uppermost mantle (10^{24} Pa s) across the Alps (Figure 3, case f) largely decreases the uplift rates (maximum rate of 0.8 mm/yr) with respect to case c (maximum rate of 1.8 mm/yr). Two processes may explain this difference: (1) the increase of plate rigidity beneath the Alps due to the addition of upper crust and uppermost mantle elastic bodies and (2) the closure of the flow connection between the low-viscosity reservoirs of the alpine lower crust and the viscous upper mantle.

The viscosity of the upper mantle has also a critical impact on present-day vertical motions. Indeed, a viscosity larger than 10^{21} Pa s induces a 200 km wide bulge and a long-lasting uplift rate (Figure 3, case e) with a maximum present-day uplift rate of 2.6 mm/yr. In addition to widen the present-day uplift, mantle viscosity significantly affects time evolution of vertical motions (Figure 4a). Indeed, a mantle viscosity of 10^{20} Pa s (Figure 3, case c) results into a high-amplitude motion during the millennia following the onset of deglaciation with a maximum uplift rate of 14 mm/yr. This time-dependent behavior is coherent with a mantle relaxation time having a Young's modulus of 10^{11} Pa and a Poisson ratio of 0.25. Increasing the mantle viscosity to 10^{21} Pa s results into a delayed response during the ice cap retreat with a maximum uplift rate reaching only 8 mm/yr (Figure 4).

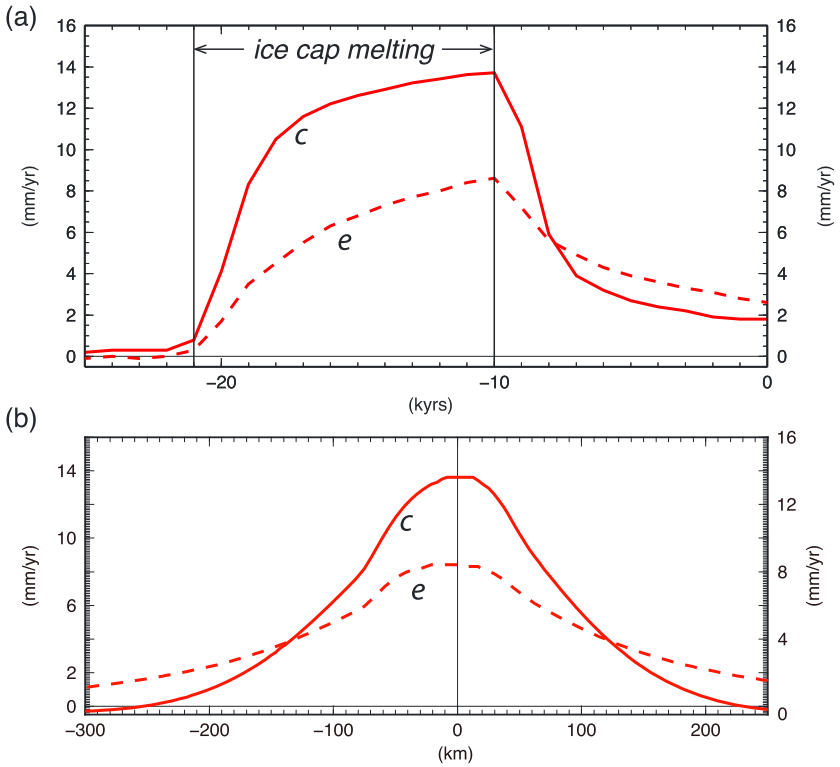

Figure 4. Temporal and spatial patterns associated with the Alpine model and influence of mantle viscosity. (a) Uplift rate evolution from −24 kyr to present for cases c and e. (b) Uplift rate distribution for cases c and e at the end of the ice retreat (−10 kyr).

4. Rheological Requirements for a Narrow Geodetic Uplift

4.1. Rheology of the Alps: An Update

We investigated the effect of a rheological heterogeneity corresponding to a low-viscosity crustal root beneath the Alps. The use of a weak crustal root creates a strain anomaly and a narrow present-day uplift of 1–3 mm/yr similar to the one revealed by geodetic measurements. As shown in Figures 3 and 5, only a combination of a crustal root viscosity lower than 10^{21} Pa s with an uppermost mantle viscosity of 10^{20} Pa s adequately fits the observations. Such a rheological layering is compatible with crustal and mantle viscosities associated to transient uplift for other continental domains [*Thatcher and Pollitz*, 2008]. For most of the reported cases, lower crustal viscosities are in the range 10^{20}–10^{21} Pa s, while mantle viscosities could be substantially lower (10^{18}–10^{21} Pa s). For example, analysis of postglacial rebound of Fennoscandia suggests mantle viscosities of 5.10^{20}–10^{21} Pa s [*Milne et al.*, 2001], but other estimates made in Southeast Alaska [*Larsen et al.*, 2005] lead to lower viscosities for the sublithospheric mantle (4.10^{18} Pa s). Modeling Alpine uplift

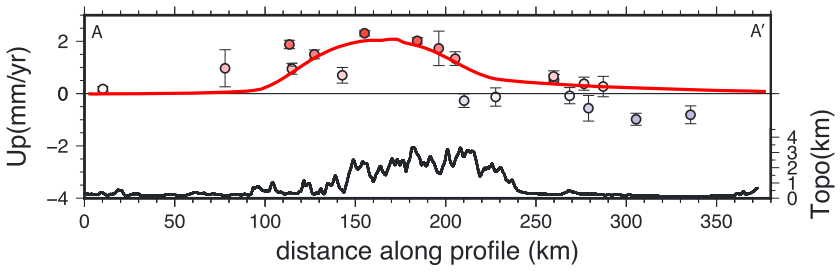

Figure 5. Uplift pattern (red curve) associated to case c (Flat model) of Table 1. Measured geodetic uplift and uncertainties along the profile located in Figure 1 are shown using colored circles; Western Alps elevation profile is given by the thick solid line below.

requires an intermediate viscosity value of 10^{20}–10^{21} Pa s. Our modeling provides a supplementary information: a high-viscosity uppermost mantle beneath the Alps does not alter the relaxation time of the system if the crustal root remains connected to the lower part of the upper mantle via a low-viscosity channel. This finding appears consistent with the high-resolution imaging of the Alps showing a disconnection between the subducting uppermost European and Ligurian mantles [*Diehl et al*., 2009]. From a rheological perspective, a 50 km wide low-viscosity channel allows an efficient crust-mantle flow. The relation between ice cap retreat, lithosphere rheology, and narrow geodetic uplift is weakly affected by the topography as shown by the "Flat model." Therefore, the combination of Holocene deglaciation over a low-viscosity body beneath the alpine topography is an appealing explanation for the observed present-day geodetic uplift. The lack of rheological heterogeneity in previously proposed postglacial rebound models of the Alps [*Stocchi et al*., 2005; *Barletta et al*., 2006] explains the failure of those studies for producing a narrow deformation signal. Our study points out the key role of a low-viscosity crustal body for triggering a narrow uplift zone following the Alpine ice cap melting, as shown recently by *Klemann et al*. [2007] for the case of southern Patagonia.

4.2. Alternate Mechanisms for a Narrow Geodetic Uplift

Our rheological model suggests that postglacial rebound could explain the Western Alps geodetic uplift. In the following, we discuss how erosion and geodynamical processes such as delamination or slab sinking may alter this uplift pattern.

1. Because of the existing relation between erosion, relief, and drainage area, alpine erosion is restricted to high topography [*Champagnac et al*., 2009]. This implies that the areas submitted to intense erosion are highly correlated with the ice cap coverage during the Pleistocene. Therefore, introducing denudation as a supplementary unloading factor is likely to produce a similar uplift pattern than the one resulting from deglaciation. Assuming local isostasy and present-day erosion rates of 0.5–1.2 mm/yr, an immediate maximum uplift of 0.4–1 mm/yr would occur. In order to quantify more thoroughly the impact of a steady state denudation, we use the rheology of case c (see Table 1) assuming a time-invariant denudation pattern ranging from 0 in the forelands to 1 mm/yr for the highest topographic part of the model. A steady state uplift having a maximum value of 0.6 mm/yr takes place, corresponding to 75% of a local isostatic rebound. If this motion superimposes to postglacial rebound associated to case c, a maximum uplift rate of 1.9–2.4 mm/yr is expected, still consistent with geodetic observations of vertical motion.
2. A traction or a torque occurring at a slab extremity has been mostly used for explaining topographic or gravimetric features of subduction [*Watts*, 2001]. Despite that the Alpine collision ended during the middle Miocene, forces related to slab detachment could be at work as suggested by some authors. These forces are probably low in magnitude because the alpine crust is close to isostatic equilibrium for the external domain of the Western Alps [*Bayer et al*., 1989]. By contrast, internal domains display large positive Bouguer anomalies indicating the presence of uplifted mantle. A comprehensive modeling including slab traction and intracrustal body forces was recently done [*Singer et al*., 2014] without showing its impact on topographic uplift.

4.3. Implication for Tectonic Activity During the Holocene

If the coda of postglacial rebound is still detectable today by continuous GNSS, uplift rates were likely much higher during ice cap melting. Using a 10^{21} Pa s for lower crustal viscosity, our model (case c) predicts an uplift rate increasing from 1 mm/yr, 21 kyr ago to 13.5 mm/yr, 10 kyr ago (Figure 4a). The average uplift rate during postglacial rebound being 10 mm/yr, a cumulated uplift of 110 m, occurred during this period, close to the local isostatic prediction of 150 m associated with the melting of a 500 m thick ice cap. If this uplift really occurred in the Alps during Holocene times, it could have altered or amplified the long-term strain rate associated with tectonic and erosional processes. A consequence of this accelerated uplift could be an extensive strain pattern corresponding to the outer bulge of the crust in a similar way to what have been proposed by *Vernant et al*. [2013] for mountain denudation. If this uplift process and extension really occurred, a brittle deformation should have affected the upper crust. In the case of the Alps, two kinds of Quaternary faults have been described so far. First, normal faulting occurs at upper crustal scale roughly perpendicular to the mountain divide as shown by both tectonic and seismological studies [*Tricart et al*., 2004; *Béthoux et al*., 2007]. At smaller scale, sackung faults took place during the Holocene in the vicinity of high topography [*Hippolyte et al*., 2009]. These faults are generally interpreted as the consequence of glacier withdrawal from alpine valleys that could have change topographic stress equilibrium (debutressing). In the Alps, cosmogenic dating

has shown that the peak of sackung fault activity occurred between 12 and 8 kyr Before Present (BP) and then progressively decreased during the Holocene. According to our model, maximum sackung activity may have occurred in response to high vertical rates associated with ice cap retreat. We propose therefore that Quaternary normal faults and sackung faults on alpine topography have been triggered by a postglacial uplift that was in turn controlled by lower crustal and upper mantle viscosities.

5. Conclusion

Our rheological model supports the idea that a significant part of the geodetic uplift of the Alps may represent the coda of a postglacial rebound occurring during the Holocene. The narrow pattern of vertical motion and its present-day amplitude require a lower crustal rheology not exceeding 10^{21} Pa s, while the uppermost mantle must have a viscosity of 10^{20} Pa s. A specific feature of this model is that a high-viscosity uppermost mantle cannot cross the plate boundary between Apulia and Eurasia because a narrow but continuous low-viscosity body must extend from the lower crust down to the lower part of the upper mantle. This particular rheological pattern is the only one matching geodetic observations, thus indicating that a combination of accurate geophysical imaging and precise geodetic observations bring key constraints on the mechanical behavior of mountain ranges.

Acknowledgments
This work has been done thanks to a CNRS-INSU grant associated with the SYSTER program. We thank J.D. Champagnac and an anonymous reviewer for their constructive comments.

References

Barletta, V. R., C. Ferrari, G. Diolaiuti, T. Carnielli, R. Sabadini, and C. Smiraglia (2006), Glacier shrinkage and modeled uplift of the Alps, *Geophys. Res. Lett.*, *33*, L14307, doi:10.1029/2006GL026490.

Bayer, R., M. T. Carozzo, R. Lanza, M. Miletto, and D. Rey (1989), Gravity modelling along the ECORS-CROP vertical seismic reflection profile through the Western Alps, *Tectonophysics*, *162*(3-4), 203–218, doi:10.1016/0040-1951(89)90244-8.

Beaumont, C., P. Fullsack, and J. Hamilton (1994), Styles of crustal deformation in compressional orogens caused by subduction of the underlying lithosphere, *Tectonophysics*, *232*, 119–132.

Béthoux, N., C. Sue, A. Paul, J. Virieux, J. Frechet, F. Thouvenot, and M. Cattaneo (2007), Local tomography and focal mechanisms in the south-western Alps: Comparison of methods and tectonic implications, *Tectonophysics*, *432*(1-4), 1–19, doi:10.1016/j.tecto.2006.10.004.

Brace, W. F., and D. L. Kohlstedt (1980), Limits on lithospheric stress imposed by laboratory experiments, *J. Geophys. Res.*, *85*, 6248–6252, doi:10.1029/JB085iB11p06248.

Brocard, G. Y., P. A. van der Beek, D. L. Bourles, L. L. Siame, and J. L. Mugnier (2003), Long-term fluvial incision rates and postglacial river relaxation time in the French Western Alps from ^{10}Be dating of alluvial terraces with assessment of inheritance, soil development and wind ablation effects, *Earth Planet. Sci. Lett.*, *209*(1-2), 197–214, doi:10.1016/S0012-821X(03)00031-1.

Burgmann, R., and G. Dresen (2008), Rheology of the lower crust and upper mantle: Evidence from rock mechanics, geodesy, and field observations, *Annu. Rev. Earth Planet. Sci.*, *36*(1), 531–567, doi:10.1146/annurev.earth.36.031207.124326.

Burov, E., Y. Podladchkov, G. Grandjean, and J. P. Burg (1999), Thermo-mechanical approach to validation of deep crustal and lithospheric structures inferred from multidisciplinary data: Application to the Western and Northern Alps, *Terra Nova*, *11*(2-3), 124–131.

Burov, E. B., and A. B. Watts (2006), The long-term strength of continental lithosphere: "Jelly sandwich" or 'crème brûlée'? *GSA Today*, *16*(1), doi:10.1130/1052-5173(2006)016<4:TLTSOC>2.0.CO;2.

Champagnac, J.-D., F. Schlunegger, K. Norton, F. von Blanckenburg, L. M. Abbühl, and M. Schwab (2009), Erosion-driven uplift of the modern Central Alps, *Tectonophysics*, *474*(1-2), 236–249, doi:10.1016/j.tecto.2009.02.024.

Deichmann, N. (2003), Focal depths of earthquakes below Switzerland, *Swiss Seismol. Serv.*, 1–4.

Diehl, T., S. Husen, E. Kissling, and N. Deichmann (2009), High-resolution 3-D P-wave model of the Alpine crust, *Geophys. J. Int.*, *179*(2), 1133–1147, doi:10.1111/j.1365-246X.2009.04331.x.

Fox, M., F. Herman, E. Kissling, and S. D. Willett (2015), Rapid exhumation in the Western Alps driven by slab detachment and glacial erosion, *Geology*, *43*(5), 379–382, doi:10.1130/G36411.1.

Gudmundsson, G. H. (1994), An order-of-magnitude estimate of the current uplift-rates in Switzerland caused by the Würm Alpine deglaciation, *Eclogae Geol. Helv.*, *87*(2), 545–557.

Hinderer, M., M. Kastowski, A. Kamelger, C. Bartolini, and F. Schlunegger (2010), River loads and modern denudation of the Alps—A review, *Earth Sci. Rev.*, *118*(C), 11–44, doi:10.1016/j.earscirev.2013.01.001.

Hippolyte, J.-C., D. Bourlès, R. Braucher, J. Carcaillet, L. Léanni, M. Arnold, and G. Aumaitre (2009), Cosmogenic ^{10}Be dating of a sackung and its faulted rock glaciers, in the Alps of Savoy (France), *Geomorphology*, *108*(3-4), 312–320, doi:10.1016/j.geomorph.2009.02.024.

Jackson, J. A., H. Austrheim, D. McKenzie, and K. Priestley (2004), Metastability, mechanical strength, and the support of mountain belts, *Geology*, *32*(7), 625–628, doi:10.1130/G20397.1.

Joó, I. (1992), Recent vertical surface movements in the Carpathian Basin, *Tectonophysics*, *202*(2-4), 129–134, doi:10.1016/0040-1951(92)90091-J.

Klemann, V., E. R. Ivins, and Z. Martinec (2007), Models of active glacial isostasy roofing warm subduction: Case of the South Patagonian Ice Field, *J. Geophys. Res.*, *112*, B09405, doi:10.1029/2006JB004818.

Lardeaux, J. M., S. Schwartz, P. Tricart, A. Paul, S. Guillot, N. Bethoux, and F. Masson (2006), A crustal-scale cross-section of the south-western Alps combining geophysical and geological imagery, *Terra Nova*, *18*(6), 412–422, doi:10.1111/j.1365-3121.2006.00706.x.

Larsen, C. F., R. J. Motyka, J. T. Freymueller, K. A. Echelmeyer, and E. R. Ivins (2005), Rapid viscoelastic uplift in southeast Alaska caused by post-Little Ice Age glacial retreat, *Earth Planet. Sci. Lett.*, *237*(3-4), 548–560, doi:10.1016/j.epsl.2005.06.032.

Lenhardt, W., C. Freudenthaler, R. Lippitsch, and E. Feigweil (2007), Focal-depth distributions in the Austrian Eastern Alps based on macroseismic data, *Aust. J. Earth Sci.*, *100*, 66–79.

Lyon-Caen, H., and P. Molnar (1989), Constraints on the deep structure and dynamic processes beneath the Alps and adjacent regions from an analysis of gravity anomalies, *Geophys. J. Int.*, *99*, 19–32.

Maggi, A., J. A. Jackson, D. McKenzie, and K. Priestley (2000), Earthquake focal depths, effective elastic thickness, and the strength of the continental lithosphere, *Geology*, *28*, 495–498.

Majorowicz, J., and S. Wybraniec (2010), New terrestrial heat flow map of Europe after regional paleoclimatic correction application, *Int. J. Earth Sci. (Geol. Rundsch)*, *100*(4), 881–887, doi:10.1007/s00531-010-0526-1.

Meissner, R., and J. Strehlau (1982), Limits of stresses in continental crusts and their relation to the depth-frequency distribution of shallow earthquakes, *Tectonics*, *1*, 73–89, doi:10.1029/TC001i001p00073.

Milne, G. A., J. L. Davis, J. X. Mitrovica, H. G. Scherneck, J. M. Johansson, M. Vermeer, and H. Koivula (2001), Space-geodetic constraints on glacial isostatic adjustment in Fennoscandia, *Science*, *291*, 2381–2385.

Nocquet, J.-M. (2012), Present-day kinematics of the Mediterranean: A comprehensive overview of GPS results, *Tectonophysics*, *579*, 220–242, doi:10.1016/j.tecto.2012.03.037.

Schaer, J. P., and F. Jeanrichard (1974), Mouvements verticaux anciens et actuels dans les Alpes suisses, *Eclogae Geol. Helv.*, *67*(1), 101–119.

Selverstone, J. (2005), Are the Alps collapsing ?, *Annu. Rev. Earth Planet. Sci.*, *33*(1), 113–132, doi:10.1146/annurev.earth.33.092203.122535.

Serpelloni, E., C. Faccenna, G. Spada, D. Dong, and S. D. P. Williams (2013), Vertical GPS ground motion rates in the Euro-Mediterranean region: New evidence of velocity gradients at different spatial scales along the Nubia-Eurasia plate boundary, *J. Geophys. Res. Solid Earth*, *118*, 6003–6024, doi:10.1002/2013JB010102.

Sibson, R. H. (1982), Fault zone model, heat flow, and the depth distribution of earthquakes in the continental crust of the United States, *Bull. Seismol. Soc. Am.*, *72*, 151–163.

Singer, J., T. Diehl, S. Husen, E. Kissling, and T. Duretz (2014), Alpine lithosphere slab rollback causing lower crustal seismicity in northern foreland, *Earth Planet. Sci. Lett.*, *397*, 42–56, doi:10.1016/j.epsl.2014.04.002.

Stocchi, P., G. Spada, and S. Cianetti (2005), Isostatic rebound following the Alpine deglaciation: Impact on the sea level variations and vertical movements in the Mediterranean region, *Geophys. J. Int.*, *162*(1), 137–147, doi:10.1111/j.1365-246X.2005.02653.x.

Sue, C., B. Delacou, J.-D. Champagnac, C. Allanic, P. Tricart, and M. Burkhard (2007), Extensional neotectonics around the bend of the Western/Central Alps: An overview, *Int. J. Earth Sci. (Geol. Rundsch)*, *96*(6), 1101–1129, doi:10.1007/s00531-007-0181-3.

Thatcher, W., and F. F. Pollitz (2008), Temporal evolution of continental lithospheric strength in actively deforming regions, *GSA Today*, *18*(4), 4, doi:10.1130/GSAT01804-5A.1.

Tricart, P., S. Schwartz, C. Sue, and J. M. Lardeaux (2004), Evidence of synextension tilting and doming during final exhumation from analysis of multistage faults (Queyras Schistes lustrés, Western Alps), *J. Struct. Geol.*, *26*(9), 1633–1645, doi:10.1016/j.jsg.2004.02.002.

Vernant, P., F. Hivert, J. Chéry, P. Steer, R. Cattin, and A. Rigo (2013), Erosion-induced isostatic rebound triggers extension in low convergent mountain ranges, *Geology*, *41*(4), 467–470, doi:10.1130/G33942.1.

Watts, A. B. (2001), *Isostasy and Flexure of the Lithosphere*, Cambridge Univ. Press, Cambridge.

Wittmann, H., F. von Blanckenburg, T. Kruesmann, K. P. Norton, and P. W. Kubik (2007), Relation between rock uplift and denudation from cosmogenic nuclides in river sediment in the Central Alps of Switzerland, *J. Geophys. Res.*, *112*, F04010, doi:10.1029/2006JF000729.